Journal of Multidisciplinary Engineering Science and Technology (JMEST)
ISSN: 2458-9403
Vol. 4 Issue 8, August - 2017

Sensorless DTC-SVM of Induction Motor by Applying Two Neural Controllers

Abdallah Farahat Mahmoud
Dept. of Electrical Engineering, Al-Azhar University, Qena, Egypt
engabdallah2012@azhar.edu.eg

Adel S. Nada
Ass. Prof. Dr. at Al-Azhar University,
Cairo, Egypt
adel.saad1@hotmail.com

Mohammed Kamal Ahmed
Ass. Prof. Dr. at Al-Azhar University,
Cairo, Egypt
mkalshaear@gmail.com

***Abstract*—Direct Torque Control (DTC) seems to be particularly interesting being independent of machine rotor parameters among all control methods for induction motor drives (IMD). In spite of its simplicity, DTC permit good torque control in both transient and steady state. The classic DTC drive utilizing a pair of hysteresis comparators. Those DTC drives suffer from the high torque, flux, stator current ripples and variable switching frequency. Using Space Vector Modulation (SVM) depends on the reference torque and flux is the most common solution to this problem. In this Paper two-neural controllers along with the SVM technique applied to the inverter to improve the performance of SVM_DTC in all round way. The rotor speed is estimated by the model reference adaptive system (MRAS) scheme which is determined from measured terminal voltages and currents. The performance of the proposed system is evaluated through digital simulation using MATLAB – SIMULINK package.**

Keywords—Induction Motor Drive; Direct Torque Control (DTC) ; Model Reference Adaptive system (MRAS); Space Vector Modulation (SVM); Neural PI Controller.

I. INTRODUCTION

The Induction motors have become widely used in the industry due to their simplicity of manufacture and maintenance. Currently, many industrial applications require control of speed, position and torque. Recent advances in power semiconductor and microprocessor technology have made possible the application of advanced control techniques to alternating current (AC) motor drive systems[1].

Nowadays, the induction machine is controlled by using many strategies. One of these strategies is direct torque control (DTC).

The main advantages of DTC are robust and fast torque response, no requirements for coordinate transformation, no requirements for PWM pulse generation and current regulators [2][3]. The major disadvantage of the DTC drive is the steady state ripples in torque and flux[4].

To minimize these problems, this paper introduces a new direct torque and flux control based on space vector modulation (DTC-SVM) for IM drives. It uses closed-loop control for both flux, torque and speed in a similar manner as DTC, but the voltage is produced by an SVM unit. In this way, the DTC transient performance and robustness are preserved and the steady-state torque ripple is reduced. Additionally, the switching frequency is constant and totally under controlled[5].

In this paper, Artificial Neural Networks based on direct torque control is proposed. Here two neural controllers for both flux and torque are proposed along with space vector modulation. The neural controllers allow faster response and SVM technique provides a constant inverter switching frequency so, small torque ripples and current distortion.

II. PRINCIPLE OF DIRECT TORQUE CONTROL

The basic functional blocks used to implement the DTC scheme in an induction motor are shown in Fig.1.

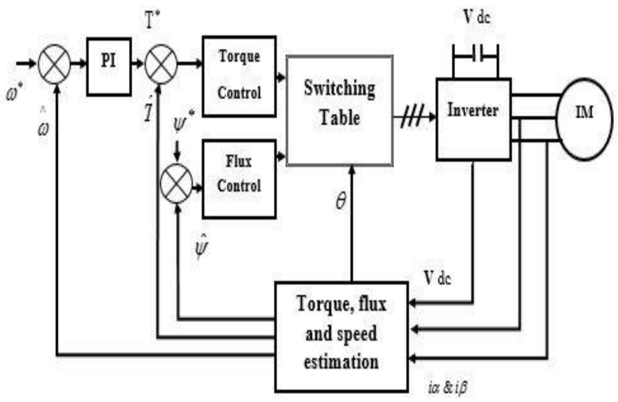

Fig. 1. *Schematic of basic sensorless DTC.*

- *Torue and flux estimator*

The feedback flux and torque are calculated from the machine terminal voltages and currents. The computation block also calculates the sector number in which the flux vector lies [6]. The phase voltage and currents in stationary reference are given as:

$$v_{s\alpha} = v_a \ and \ v_{s\beta} = \frac{1}{\sqrt{3}}(v_a + 2v_b) \quad (1)$$

$$I_{s\alpha} = I_a \; and \; I_{s\beta} = \frac{-1}{\sqrt{3}}(I_a + 2I_b) \qquad (2)$$

Where

$v_{s\alpha}$, $v_{s\beta}$	Are α -axis and β -axis stator voltage components
v_a , v_b	Are the phase voltage 'a' 'b'.
$I_{s\alpha}$, $I_{s\beta}$	Are α -axis and β -axis stator current components
I_a , I_b	Are the phase currents 'a' 'b'.

The components of stator flux are given by:

$$\varphi_{s\beta} = \int (v_{s\alpha} - R_s I_{s\alpha})dt \qquad (3)$$

$$\varphi_{s\beta} = \int (v_{s\beta} - R_s I_{s\beta})dt \qquad (4)$$

The magnitude of the stator flux can be estimated by:

$$\varphi_s = \sqrt{{\varphi_{s\alpha}}^2 - {\varphi_{s\beta}}^2} \qquad (5)$$

Where

$\varphi_{s\alpha}$, $\varphi_{s\beta}$	Are $\alpha -$ axis and β -axis stator flux linkage components.
R_s	Is the stator resistance.
φ_s	Is the stator flux.

The flux vector zone can be obtained using the stator flux components .By using the flux components, current components and IM number of poles, the electromagnetic torque can be calculated by:

$$T_e = \frac{3}{2}\frac{p}{2}(\varphi_{s\alpha} I_{s\beta} - \varphi_{s\beta} I_{s\alpha}) \qquad (6)$$

Where

T_e	Is the electromagnetic torque.
p	Is the number of pole pairs.

- *Torque and flux controller*

The instantaneous values of flux and torque are calculated from stator variables by using flux and torque estimator. The command stator flux φ^* and torque T_e^* magnitude are compared with their respective estimated values and the errors are processed by the hysteresis band stator flux controllers and hysteresis band electromagnetic torque controllers The flux loop controller has two levels of digital output according to following equations.

$$H_\varphi = 1 \quad for \; E_\varphi > +HB_\varphi \qquad (7)$$

$$H_\varphi = -1 \; for \; E_\varphi > -HB_\varphi \qquad (8)$$

The total hysteresis band width of the flux loop controller is $2HB_\varphi$. The actual stator flux is constrained within the hysteresis band and tracks the command flux. The actual stator flux is constrained within this band and it tracks the command flux in zigzag path as shown in Fig.2 [7].

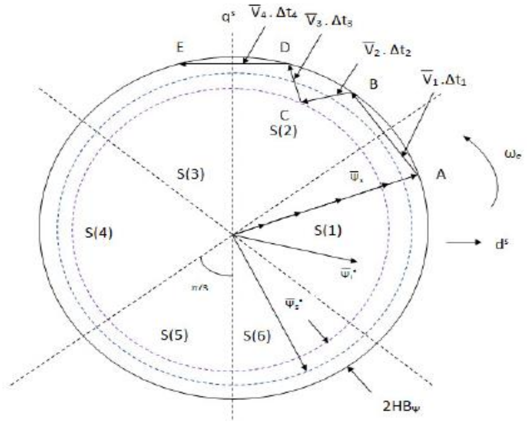

Fig. 2. *Inverter Trajectory of stator flux vectors.*

The torque control loop has three levels of digital output represented by the following equations:

$$H_T = 1 \quad for \; E_T > +HB_T \qquad (9)$$

$$H_T = -1 \; for \; E_T > -HB_T \qquad (10)$$

$$H_T = 0 \; for -HB_T < E_T < +HB_T \qquad (11)$$

- *Switching table*

The switching selection block in Fig.1, receives the input signals H_φ , H_T and $s(k)$ and generate the desired control voltage vector as given in look-up table shown in Table 1.

TABLE I. SWITCHING TABLE OF INVERTER VOLTAGE VECTOR

H_φ	H_T	S_1	S_2	S_3	S_4	S_5	S_6
1	1	V_2	V_3	V_4	V_5	V_6	V_1
	0	V_0	V_7	V_0	V_7	V_0	V_7
	-1	V_6	V_1	V_2	V_3	V_4	V_5
-1	1	V_3	V_4	V_5	V_6	V_1	V_2
	0	V_7	V_0	V_7	V_0	V_7	V_0
	-1	V_5	V_6	V_1	V_2	V_3	V_4

The inverter voltage vectors and a typical φ_s are shown in Fig.3. Neglecting the stator resistance R_s of the machine, we can write

$$V_S = \frac{d}{dt}(\varphi_S) \quad \text{or} \quad \Delta\varphi_S = V_S.\Delta t \qquad (12)$$

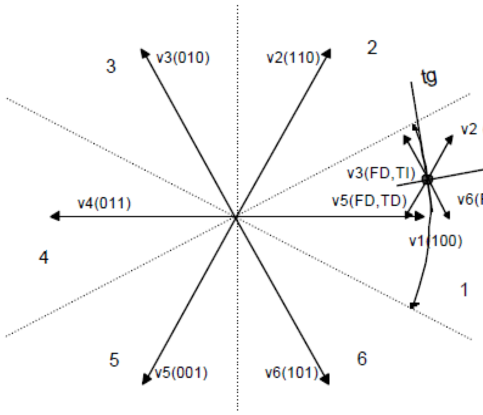

Fig. 3. *Inverter Voltage vectors and corresponding stator flux variation caption.*

- *Speed estimation*

Sensorless drives are becoming more and more important as they can eliminate the speed sensor maintaining accurate response. Monitoring only the stator current and stator voltages, it is possible to estimate the necessary control variables. The observer type used here is a model reference adaptive system (MRAS).

The MRAS principle is based on the comparison of two estimator's outputs. The first is independent of the observed variable named as model reference. The second is the adjustable one. The error between the two models feeds an adaptive mechanism to turn out the observed variable[8].

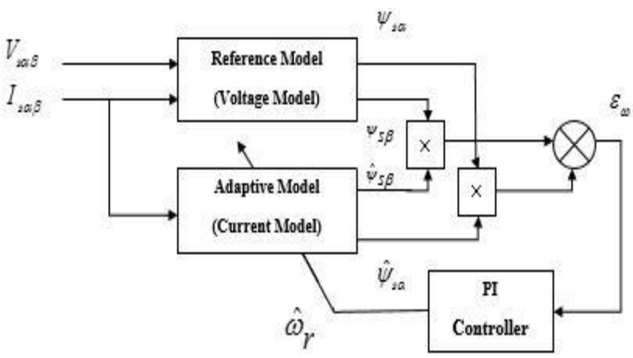

Fig. 4. *Model reference adaptive system.*

- Reference model

The reference rotor flux components obtained from the reference model are given by:

$$\psi_{r\alpha\beta} = \frac{L_r}{L_m}(\int([v_{s\alpha\beta}] - r_s[i_{s\alpha\beta}])\,dt - \sigma L_s[i_{s\alpha\beta}] \qquad (13)$$

- Adaptive model

It explicitly depends on speed and will be constructed from equations of the machine rotor parameters as:

$$\hat{\psi}_{r\alpha\beta} = \int[(-\frac{1}{T_r} + j\omega_r)[\hat{\psi}_{s\alpha\beta}] + \frac{L_m}{T_r}[i_{s\alpha\beta}]]\,dt \qquad (14)$$

- Error between two models

Finally the adaptation scheme generates the value of the estimated speed to be used in such a way as to minimize the error between the reference and estimated The expressions for the speed tuning signal and the estimated speed can be given as:

$$\varepsilon_\omega = I_m(\bar{\psi}_r \cdot \hat{\bar{\psi}}_r^{\,*}) = (\psi_{r\beta}\psi\hat{\psi}_{r\alpha} - \psi_{r\alpha}\hat{\psi}_{r\beta}) \qquad (15)$$

$$\hat{\omega}_r = k_p\,\varepsilon_\omega\Big| + k_i\int\varepsilon_\omega dt \qquad (16)$$

III. PRINCIPLE OF DTC-SVM

The basic functional blocks used to implement the DTC-SVM scheme is shown in Fig.5.

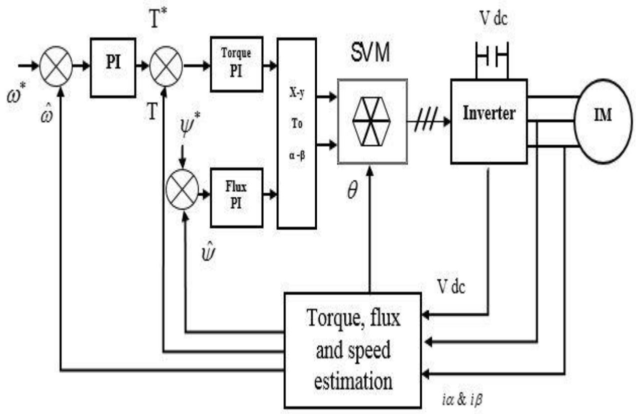

Fig. 5. *Schematic of sensorless DTC-SVM.*

In the proposed system, flux and torque estimators are used to determine the actual value of the flux linkage and torque. Instead of the switching table and hysteresis controllers, a Proportional-Integral (PI) controller and numeric calculation are used to determine the duration time of voltage vectors, such that the error vector in flux and torque can be fully compensated. Two proportional integral controllers regulate the flux and torque error.

Since the controllers produce the voltage command vector, appropriate space voltage vector can be generated with SVM and a fixed switching frequency can be achieved. The output of the PI flux and torque controllers can be interpreted as the reference stator voltage components in d-q coordinate system. These DC voltage commands are then transformed into the stationary frame (α-β), the command values v_α, v_β are delivered to SVM block. The SVM block performs the space vector modulation of V_s to obtain the gate drive pulses for the inverter circuit[6].

- Space vector modulation

Space vector modulation SVM technique involves eight rules for switching modes of inverter to control the stator flux to move with the reference flux vector in a circle. It achieves the highest controlling. Eight types of switching modes are corresponding respectively to eight space voltage vectors that contain six active voltage vectors and two zero voltage vectors. The axes of hexagon contain six active voltage vectors, and at the origin, there are two zero voltage vectors. All these are the basic space vectors. Shortly the SVM-DTC method selects one of the six nonzero and two zero voltage vectors of the inverter on the basis of the instantaneous errors in torque and stator flux magnitude. These sectors are shown in Fig.6. [5].

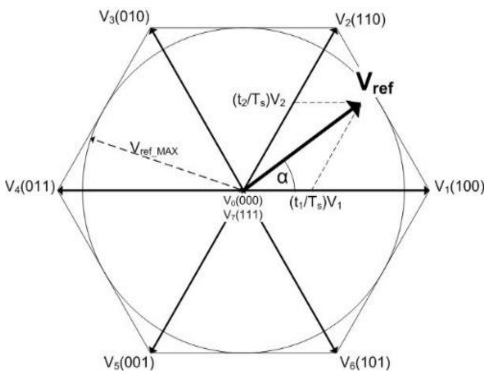

Fig. 6. *Switching vectors and sector caption.*

Space vector PWM can be implemented by the following steps:

1) Transform three phase to two phase quantity and determine V_s and angle δ.

2) Determine time duration T_1, T_2 and T_0.

3) Calculation of switching time for each switch.

IV. DTC-SVM WITH ANN CONTROLLERS

The complete block diagram SVM-DTC induction motor drive with two ANN controllers are shown in fig.7. The PI controllers are being replaced by ANN controller to get better response in stator current, speed, torque and flux.

The algorithm operates with two ANN Controllers for decoupled flux and torque control. Torque error and flux error are taken as input to ANN. A two hidden layer neural network been used in this system. The structure has fifteen neurons in the in the first layer and one neuron in the second layer. Both the controllers produce a stator voltage vector component, which, forms control voltage vector in rectangular form. This is further synthesized by SVM unit and applied to IM through VSI.

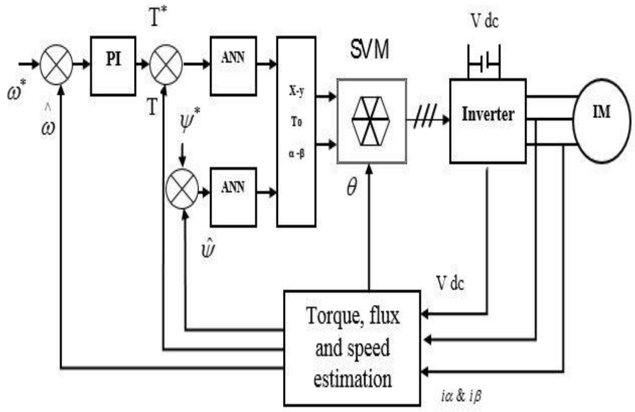

Fig. 7. *Block diagram of sensorless SVM-DTC with two ANN controller.*

V. SIMULATION MODEL OF DTC-SVM.

A direct torque control algorithm of Induction motor drive has been simulated using MATLAB/SIMULINK. The base of stator current is 12.3 A, stator flux linkage is taken as 0.3 Wb, load torque applied is 12.53 Nm and 1705 rpm for the speed. Figure 8 shows Simulink model of sensorless DTC-SVM for induction motor drive

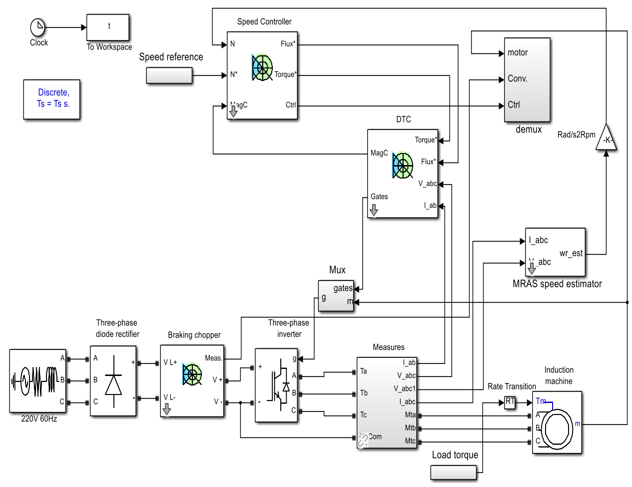

Fig. 8. *Simulink model of sensorless DTC-SVM scheme of IM.*

VI. SIMULATION RESULTS

1) Stator current

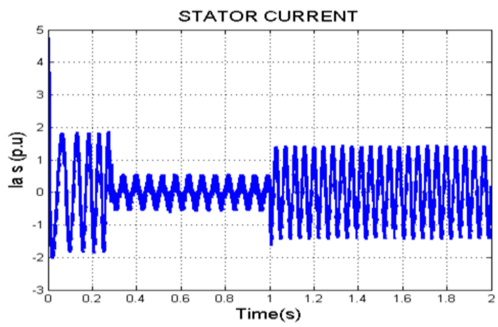

Fig. 9. *Stator phase 'a' current vs. time of classic-DTC.*

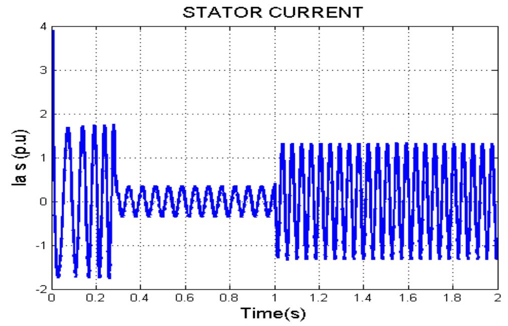

Fig. 10. *Stator phase 'a' current vs. time of (DTC-SVM).*

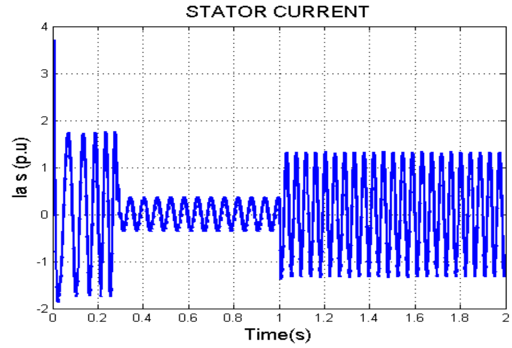

Fig. 11. *Stator phase 'a' current vs. time of (DTC-SVM) with ANN controller.*

Figure 9 shows Stator current in p.u for classical DTC, which has considerably very high ripple, while Fig. 10 shows Stator current in p.u for DTC-SVM which has a minimum value of ripple. Fig.11 shows Stator current in per unit for DTC-SVM with two ANN controllers. The magnitude of stator current fluctuations at last two cases is nearly the same. But the stator current in the second case tends to sinusoidal wave under faster speed. The difference of the stator current is not obvious in steady state in both cases.

2) *Stator flux*

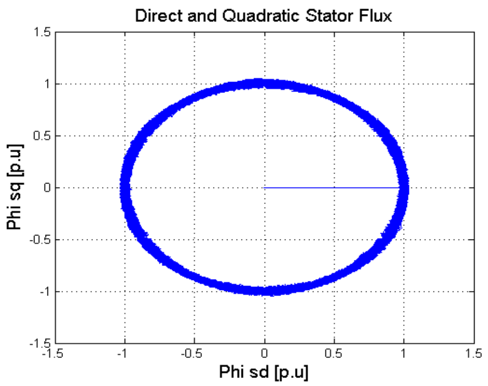

Fig. 12. *Stator 'q' and 'd' flux linkages of classic - DTC.*

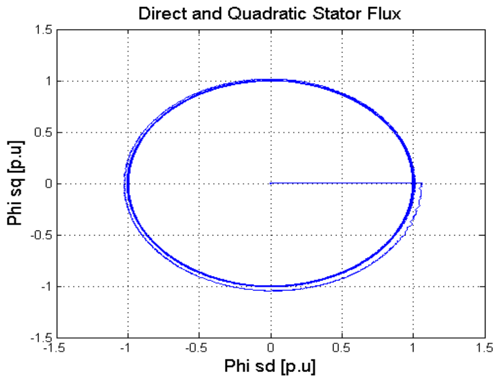

Fig. 13. *Stator 'q' and 'd' flux linkages of (DTC-SVM).*

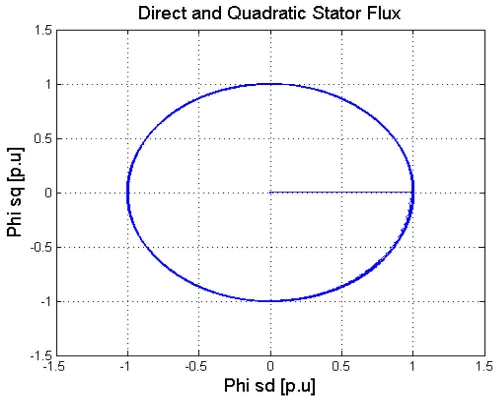

Fig. 14. *Stator 'q' and 'd' flux linkages of (DTC-SVM) with ANN controller..*

Figure 12 shows Stator flux circle in p.u for classical DTC, which has a large value of ripple around 0.07 p.u, while Fig.13 shows Stator flux circle in p.u for DTC-SVM which has a minimum value of ripple compared to the classic DTC, the value of ripple around 0.012 p.u. Fig.14 shows stator flux circle in p.u for DTC-SVM with two ANN controllers which has better performance than the DTC-SVM schema with PI controllers.

3) *Electromagnetic torque*

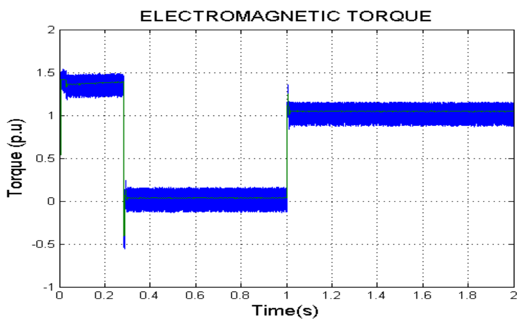

Fig. 15. *Electromagnetic torque vs. time of Classic-DTC.*

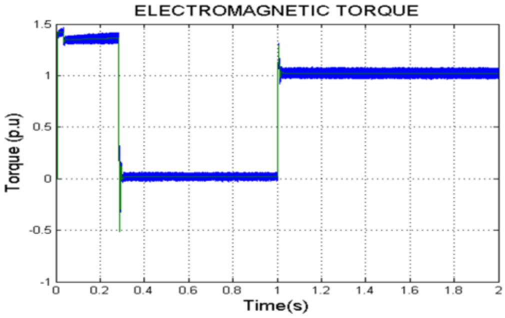

Fig. 16. *Electromagnetic torque vs. time of (DTC-SVM).*

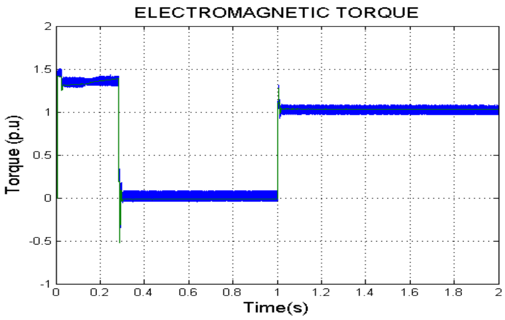

Fig. 17. *Electromagnetic torque vs. time of (DTC-SVM) with ANN controller.*

Figure 15 shows the electromagnetic torque in p.u for the classical DTC, which has an unaccepted ripple value of torque 0.265 p.u. Fig.16 shows electromagnetic torque in p.u for DTC-SVM. The ripple value of torque was reduced and became 0.1 p.u which is an accepted. Fig.17 shows electromagnetic torque in per unit for DTC-SVM with two ANN controllers, which has faster responses at changing of speed and electromagnetic torque.

4) Comparisons Between DTC-SVM with PI & ANN Controller

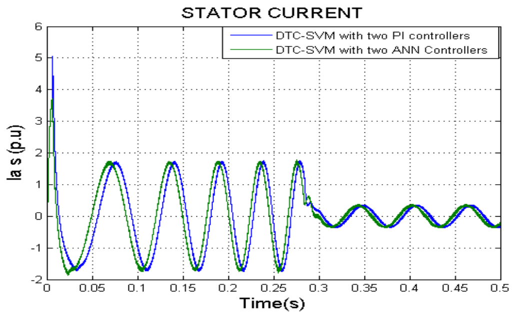

Fig. 18. *Stator phase 'a' current vs. time.*

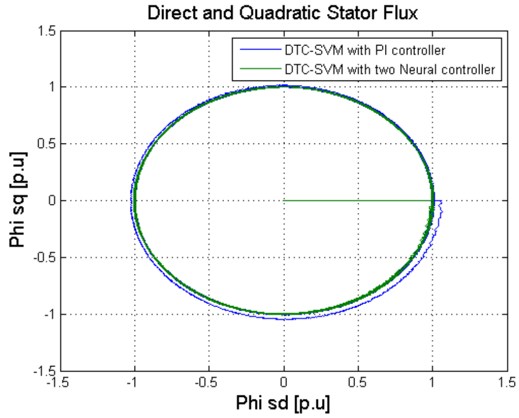

Fig. 19. *Stator 'q' and 'd' flux linkages.*

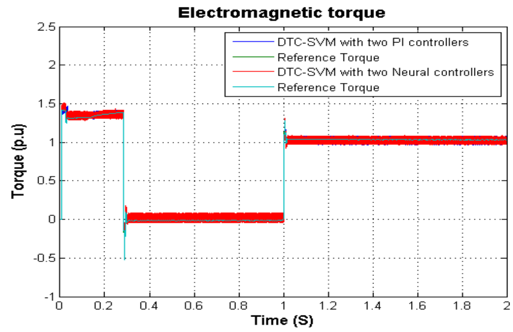

Fig. 20. *Electromagnetic torque vs. time.*

5) Speed Estimation

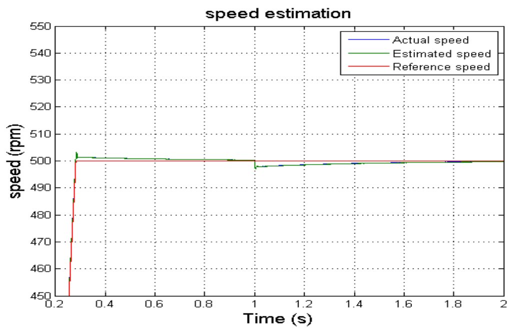

Fig. 21. *Operation at various speeds; reference, actual and estimated speed.*

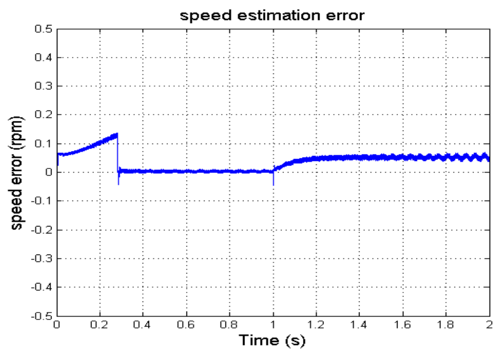

Fig. 22. *Operation at speed estimation error.*

VII. CONCLUSION .

In this paper a new space vector modulation based direct torque control technique with neural controllers were proposed. The main focus of this paper is to minimize the high ripples of torque, flux and stator current in the conventional DTC. The proposed control technique has been modeled and simulated in the MATLAB/SIMULINK environment. The simulation results proved that the superiority of the proposed control technique by reducing of the torque ripples about 62% and about 82% for the flux ripples. The SVM preserves constant switching frequency and ANN technique achieved fast stator current, flux and electromagnetic torque response in a transient state.

VIII. SPECIFICATION OF INDUCTION MOTOR

TABLE II. SPECIFICATION OF MOTOR

Parameter	**Value**
Power	2238 VA
Rated voltage	220 V
Pole pairs	2
Frequency	60 HZ
Phase	3
Stator leakage inductance	0.002 H
Rotor leakage inductance	0.002 H
Stator mutual inductance	0.0693 H
Rotor inertia	0.089(Kgm^2)
Rotor friction	0.005 (Nms)
Stator resistance	0.435 Ω
Rotor resistance	0.516 Ω

IX. REFERENCES

[1] M. A. Chiali El Mehdi, Meroufel Abdelkader, Guebli Abderrahmane, "Sensorless Direct Torque Control of Induction Machine with MRAS Speed Estimator," Computer Science and Engineering, Vol. 3(1), pp. 8-13, 2013.

[2] M. Depenbrock, "Direct Self-Control (DSC) of Inverter-Fed Induction Machine," IEEE transactions on Power Electronics, Vol. 3, pp. 420-429, 1988.

[3] P. Tiitinen and M. Surandra, "The Next Generation Motor Control Method, DTC Direct Torque Control," in Power Electronics, Drives and Energy Systems for Industrial Growth, 1996., Proceedings of the 1996 International Conference on, pp. 37-43, 1996.

[4] P. Marino, M. D'incecco, and N. Visciano, "A Comparison of Direct Torque Control Methodologies For Induction Motor," in Power Tech Proceedings, 2001 IEEE Porto, p. 6 pp. Vol. 2, 2001.

[5] Hafeezul Haq1, Mehedi Hasan Imran1, Halil Ibrahim Okumus1, Zia-ul-Haq2, "SVM and PI Based Simplest Approach to Direct Torque Control of Induction Motor," International Journal of Electronic Engineering and Computer Science, Vol. 1, pp. 1-5, 2016.

[6] A. Manuel and J. Francis, "Simulation Of Direct Torque Controlled Induction Motor Drive By Using Space Vector Pulse Width Modulation For Torque Ripple Reduction," International Journal of Advanced Research in Electrical, Electronics and Instrumentation Engineering, Vol. 2, 2013.

[7] T. Siraj Ahmed, S. Sao, and K. Anjaneyulu, "DTC of Twelve Sector IM Drive Using Four Level Hysteresis Control to Reduce Torque Ripple Comparing with Conventional Control," International Journal of Engineering Research and Applications, Vol. 3, pp. 115-120, 2013.

[8] M. R. Douiri, T. Nasser, A. Essadki, and M. Cherkaoui, "Direct Torque Control Of Induction Motor Based On Artificial Neural Networks With Estimate And Regulation Speed Using The MRAS And Neural Pi Controller," Journal of Theoretical & Applied Information Technology, Vol. 20, 2010.